

AD-A067 897

NAVAL SURFACE WEAPONS CENTER DAHLGREN LAB VA
MODELING OF MICROWAVE RECTIFICATION RFI EFFECTS IN LOW FREQUENC--ETC(U)
1977 R E RICHARDSON

F/G 20/14

UNCLASSIFIED

NL

[OF]
AD
A067897



END
DATE
FILMED

6 --79
DDC

DDC

APR 25 1979

B

MODELING OF MICROWAVE RECTIFICATION RFI EFFECTS IN LOW FREQUENCY CIRCUITRY

Dr. Robert E. Richardson, Jr.
US Naval Surface Weapons Center
Dahlgren, Virginia 22448

ABSTRACT

This paper discusses the rectification response exhibited by low frequency bipolar transistors when microwave energy is injected. A circuit analysis model for calculating low frequency small signal response to microwave energy is discussed and applied in analyzing the behavior of a 741 op-amp.

Quantitative theoretical calculations are performed to relate the response of a small NPN transistor similar to that used in a 741 op-amp to its material and geometrical parameters.

INTRODUCTION

It has been found that spurious microwave signals may be rectified in low-medium F_T bipolar transistors producing a shift in their quiescent operating (Q) point, and resultant circuit malfunction. Classic examples of this effect are pacemaker malfunction near a microwave oven or electronic brake control malfunction near a high power mobile transmitter. For low level microwave injection into a device, square law envelope detection occurs where a low frequency signal is produced which is proportional to the microwave power absorbed in the device.

This paper briefly describes a model for calculating the magnitude of an RF-induced offset voltage at the emitter-base junction of a transistor in terms of the absorbed RF power and device geometrical and material parameters. The model is then applied in analysis of the behavior of a 741 op-amp and comparison is made between measured and experimental results.

BASIC EFFECTS

An RFI test circuit for a transistor or IC is shown in Figure 1.⁽¹⁾ With this circuit, a known amount of RF/microwave energy is injected into the device under test and the change in DC/video or quiescent operating conditions are observed. The microwave and DC impedance or termination can be independently controlled so that the device exists in a given specified environment for both in band and microwave parameters.

A transistor mounted in a circuit similar to that shown in Figure 1 exhibits a change in emitter-base voltage and in collector current when microwave energy from the source V is applied. The behavior of average collector current is dependent upon the value of Thevenin resistance R_{TH} in the base supply circuit. Small values of R_{TH} allow the collector current to increase when power is applied while high values which maintain a constant base current allow a decrease in collector current when RF power is applied. The increase in collector current observable when a low base supply Thevenin impedance is employed is understandable in terms of a standard one-dimensional, non-linear model which predicts an offset voltage at the emitter base junction due to the non-linearity of its I-V characteristic. The decrease in collector current which is generally observed in circuitry where the Thevenin impedance is high is due additionally to AC crowding and

non-uniformity of gain across the emitter. In an emitter follower circuit such as that which appears at the 741 input, the principle circuit response is due to the emitter-base offset voltage, which may be calculated from knowledge of device material and geometrical factors.

RF Rectification Model

Measurements and calculations have shown that rectification in a bipolar transistor operating in a linear active mode occurs principally at the emitter-base junction. Further, as long as the RF voltage (V) at the junction is not significantly greater than 26 mV, the rectified offset voltage (ΔV) follows a square law relationship and is proportional to the absorbed RF power. In this mechanism, (square law rectification) the offset voltage is basically proportional to the second derivative (non-linearity) of the I-V characteristic and to the square of the RF voltage (V).

The DC offset voltage ΔV at a PN junction due to an impressed RF voltage of rms value V is given by:

$$\Delta V = \frac{\hat{V}^2}{2V_T} = \hat{V}^2 \frac{1}{2(.026)} \text{ Volt} \quad (1)$$

where: $V_T = \frac{kT}{q} = .026 \text{ volt}$

The emitter-base junction may be modelled as an RC transmission line^(3,4) as shown in Figure 2, with parameters \bar{R} and \bar{C} determined by device doping and geometrical factors. Particularly important are the emitter-base junction capacitance per unit area (C_π/A_E) and the base sheet resistivity (R_S) which is determined by the resistivity (ρ_B) of the base region and the base width (W_B). The emitter perimeter (P_E) is also important. For combinations of the above parameters and frequency (ω) such that there is AC crowding (a condition which is met in a 741 input transistor at 1 GHz), the input impedance of the transmission line representing the junction is given by:

$$Z_i = \sqrt{\frac{\bar{R}}{j\omega\bar{C}}} = \sqrt{\frac{1}{j\omega} \cdot \frac{A_E}{C_\pi} \cdot R_S \cdot \frac{1}{P_E^2}} \text{ (Ohm)}$$

where: $\bar{R} = R_S \frac{1}{P_E}$ $\bar{C} = C_\pi \frac{P_E}{A_E}$ (2)

For the small input transistor at the input of a 741 we use the parameter values:

$$R_S = 4 \times 10^3 \text{ ohms/square} = \rho_B/W_B$$

$$C_\pi = 3 \times 10^{-12} \text{ farad}$$

$$A_E = 1.92 \times 10^{-5} \text{ cm}^2$$

$$P_E = 1.77 \times 10^{-2} \text{ cm}$$

*Work supported by NSWC IR funds and NAVEX Res. & Tech. Dir. Task X54.585/B02

DISTRIBUTION STATEMENT A

Approved for public release;
Distribution Unlimited

U.S. Government work not protected by U.S. copyright.

391 598

79 04 26 378

mt

DDC FILE COPY, AD A067897

With these numbers the junction input impedance at 1 GHz is calculated as $Z_j = 154 \frac{1-j}{\sqrt{2}} \Omega$

Neglecting RF power losses at all points in the device except at the emitter-base junction, the RMS RF junction voltage V^2 for a given absorbed power P_A is:

$$V^2 = P_A \frac{|Z_j|^2}{R_j} \text{ Volt}^2 \quad (3)$$

where $R_j = R_e \quad Z_j$

Combining this with (1) and (2) we obtain:

$$\frac{\Delta V}{P_A} = \frac{q}{\sqrt{2kT}} \sqrt{\frac{P_A}{W_b} \cdot \frac{A_b}{\omega C_v} \cdot \frac{1}{P_e}} \quad (\text{Volt/Watt}) \quad (4)$$

Typically, for small transistors such as are used in a 741, $\Delta V/P_A$ is several kilovolts per absorbed watt of microwave power indicating that microwatt levels of RF are sufficient to cause millivolt levels of RFI.

The rectified voltage ΔV appears in series with the base lead and a fraction (X) of emitter area (Figure 3) or total emitter current assuming uniform current density, given by:

$$X = \frac{P_e}{A_e \cdot 2 \sqrt{F R C}} \quad (5)$$

The fraction X of area is the equivalent region around the emitter perimeter excited by RF which decreases exponentially with distance toward the center, divided by the total emitter area. The collector current reduction observed in common-emitter circuits with high base circuit impedance occurs because the voltage ΔV increases the emitter edge bias and decreases the bias at the central portion of the emitter, thus redistributing the emitter bias current density toward the edge. The current gain at the emitter edge (β_E) is lower than at the center (β_C) because of fringing effects and surface recombination at the Si:SiO₂ interface; so for a constant base current, the collector current decreases when ΔV is present. The redistribution together with gain variation across the emitter is thus responsible for rectification effects which have been reported earlier⁽¹⁾. Depending upon the circuit application, either the current reduction effect or the voltage offset effect may be more important.

RFI Sensitivity and Device Size

Equation (4) yields the rectified offset interference voltage ΔV at the emitter-base junction of a transistor per unit absorbed RF power, in terms of device material and geometrical factors. It is particularly interesting to note the inverse relationship between sensitivity to rectification RFI, as evidenced by a high value of $\Delta V/P_A$, and the emitter perimeter P_e .

Choosing typical values of doping and base width, the line shown in Figure (4) for $\Delta V/P_A$ vs emitter

perimeter at a fixed frequency of 300 MHz is calculated, and measured values of the offset voltage per unit absorbed power at 300 MHz on several devices have been added for comparison. Clearly, small devices are more susceptible to rectification effects since they tend to have a higher junction impedance for a given set of doping and current density conditions. With current photoresist-based technology, the minimum line width of 2-3 micrometers means that an emitter perimeter of about 10 micrometers is feasible in an IC device. Therefore, future RFI sensitivity will probably become significantly greater than it is now, even before the occurrence of any major changes in technology other than the greater use of ion implantation which allows the realization of small line widths in practical circuits.

741 Op-Amp Behavior in the Presence of Rectification RFI

For measurement purposes, Op-amps have been tested^(6,7) in circuitry similar to that shown in Figure 1. A known amount of RF power can be injected into any of the device terminals and the resultant change in DC or video voltages is observed. The output voltage (V_o) typically varies in a manner similar to that shown in Figure 5 as the absorbed RF power is increased. V_o shows variation whether the RF is injected at one of the inputs, an offset port or even the output port. Certain ports such as the input or bias offset ports generally tend to be more sensitive. The response shows symmetry which is related to device symmetry. For example, the response with RF power injected into the inverting input is opposite and nearly equal in magnitude to the response with an equal amount of power injected into the non-inverting input. This response symmetry is useful in RFI cancellation efforts⁽⁸⁾.

As shown in the data of Figure 5, the change in output voltage V_o is proportional to absorbed power (Figure 5 is semi log) for low power levels. At higher levels the proportionality breaks down with the output voltage changing in more or less random fashion, due to large signal or saturation effects. The analytical portion of this paper is limited to the low level regime as indicated by the calculation line in Figure 5. At low levels, the square law rectification model can be expected to hold and quantitative 741 response estimates can be made.

Interference Circuit Analysis

In order to analyze the type of data shown in Figure 5, the RF interaction model described earlier was employed in 741 circuitry and subjected to circuit analysis.

While a 741 circuit as shown in Figure 6 could have been analyzed directly using large circuit analysis programs, the circuit was simplified to that shown in Figure 7 for analysis. The simplified topology retains the structure of the input circuitry however, which is desirable if one is testing the correctness of an RF interaction model on a microscopic level. For general RFI circuit analysis, one may prefer to use a macromodel⁽⁵⁾ which is perhaps somewhat easier to implement.

The overall circuit gain of 230K for this device was arrived at by choosing the stages of Figure 7 to have voltage gains of 239, 962 and +1 respectively to approximate those of the real design.

Using the material and doping parameters given for small NPN 741 input transistors, the 1 GHz RFI model parameters are:

$$\frac{\Delta V}{P_A} = 3.1 \times 10^3 \text{ volt/watt}$$

$$x = 0.33^*$$

$$\text{with } \beta_E = 90, \beta_C = 180$$

The RFI model was then substituted into the circuit of Figure 7 which was imbedded in a 10X resistive network of Figure 5. RFI at different locations in the model was simulated by activating the source ΔV in any of the transistors Q_1 , Q_2 , Q_5 or Q_6 and calculating the results with the network analysis program NET-2.

A very simple analysis of RF effects may be conducted assuming that ΔV acts in series with the input transistor at the inverting input. It may be noted that if $X = 1.0$ in the model, exactly this condition results where ΔV is equivalent to an effective offset voltage (V_{i1}) referred to the input as shown in Figure 8 and:

$$\Delta V_O = -\Delta V [1 + R_F/R_I] = -11 \Delta V \quad (7)$$

This calculation should form an estimate of the circuit response for the cases analyzed with the RFI in the input and bias offset transistors. NET-2 calculations showed that:

$$\Delta V_O = \pm 8.85 \Delta V \text{ RF @ I or NI ports } Q_2 \text{ or } Q_1$$

$$\Delta V_O = \pm 11.48 \Delta V \text{ RF at Bias offset ports } Q_5 \text{ or } Q_6$$

Apparently, because of circuit interaction between Q_5 and Q_6 , the circuit is slightly more susceptible to RFI at the bias offset ports than predicted by the single placement of ΔV at the input. Why this is so is not immediately obvious.

Difficulty in interpreting results from RFI measurements on integrated circuits often occurs because of the complicated paths the RF energy may take when it enters the chip. RF energy injected into the inverting input transistor Q_2 in Figure 6 may be partially absorbed in Q_8 or Q_4 as well as Q_2 . Some RF may even be absorbed in another transistor on the chip which has a metalization path that runs near that of Q_8 for example.

Fortunately these effects are not always severe since RFI effects often cancel by common mode rejection in the circuit for example in Q_7 or Q_8 or Q_9 , but they make analysis difficult.

Comparison of Measurements and Calculation

The effective offset voltage V_{i1} in Figure 5 or

*Numerical calculations based upon slightly different device material parameters utilized
 $X = 0.8$

8 measured for devices is less than that predicted for the 741 ΔV calculation. This may be due to slightly inaccurate estimates of device material parameters but is probably due mostly to RF being absorbed in regions of the IC where rectification either does not occur or is not important. Figure 8 shows measured small signal offset voltages at different frequencies.* The roll-off of RFI sensitivity with frequency is considerably more rapid than predicted by the analytical interaction model which neglects power loss at any point except the emitter-base junction. Other calculations show that absorption in the base-collector overlap region outside the active emitter should become important at about 1.5 GHz.

OTHER EFFECTS

In RFI measurement on 741 IC's⁽⁶⁾ it was found that at some frequencies the devices were susceptible to RF power injected on the output⁽⁵⁾ terminal as they were to RF power injected at the input or bias offset ports. In retrospect at least, this is not surprising. A feedback path from Q_{25} (which according to the behavior outlined initially should turn on harder in the presence of RFI since R_{10} is small) exists through the current mirror Q_{22} Q_{23} . An increase in collector current Q_{25} pulls the base voltage of Q_{16} down increasing the collector voltage of Q_{17} thus driving the output voltage (Q_{15} & Q_{25} emitters) more positive, as was observed in measurements.

That such effects can occur is important to keep in mind since one might be tempted, because of space or other requirements, to use less shielding or bypassing at the output of a circuit than at the input.

SUMMARY

Microwave rectification effects in bipolar transistors have been discussed quantitatively and a rectification model has been applied in analysis of RFI data on 741 operational amplifiers. Calculations of device behavior from 1 GHz RF are in basic agreement with measurements, although at higher frequencies the devices are progressively less susceptible than indicated by the calculations, which neglect RF absorption in parasitic region of the device.

The RF interaction model shows that for a given set of material parameters, the susceptibility of a device varies inversely with its size. Small, high speed devices show 1 GHz rectification sensitivity factors of about 3×10^3 V/W indicating that microwatt levels of spurious RF energy are sufficient to cause millivolt levels of RFI.

REFERENCES

1. R. E. Richardson, V. G. Puglielli, R. A. Amadori, "Microwave Interference Effect in Bipolar Transistors". IEEE Transactions on Electromagnetic Compatibility Vol EMC-17 No. 4, Nov 1975.

*Reduction of data (5) by a different technique (6) yields somewhat greater (10 dB) sensitivity estimates for the device.

79 04 26 378

Doc.	or SPECIAL
A	

2. H. C. Torrey and C. A. Whitmer, Crystal Rectifiers, Boston Technical Publishers, Inc., Lexington, Mass. (1964).
3. R. L. Pritchard, "Two Dimensional Current Flow in Junction Transistors at High Frequencies". Proc IRE Vol 46 pp 1152-1160, June 1958.
4. R. E. Richardson, Jr. "Small Signal Rectification Response of Bipolar Transistors to AC Excitation" to be published.
5. G. R. Boyle, B. M. Cohn, D. O. Pederson and J. E. Solomon "Macro Modeling of Integrated Circuit Operational Amplifiers". IEEE Journal of Solid-State Circuits Vol SC-9 No. 6, December 1974.
6. "Integrated Circuit Electromagnetic Susceptibility Investigation Phase II" Bipolar Op-Amp Study (MDC-E1124) 9 August 1974, Prepared under contract number N00178-73-C-0362 for the US Naval Weapons Laboratory, by McDonnell Douglas Astronautics Co - East, St. Louis, MO.
7. Integrated Circuit Electromagnetic Susceptibility Investigation - Phase III Summary Report No. 2, MDC-E1168. Submitted to the contracting officer, US Naval Surface Weapons Center, Dahlgren, Virginia under contract No. N60921-76-C-A030. By McDonnell Douglas Astronautics Co - East, St. Louis, MO.
8. R. E. Richardson, Jr. "RF Interference Cancellation in Low Frequency Differential Amplifiers", U.S. Navy Technical Disclosure Bulletin Vol. 1 #8, Dec 1976.

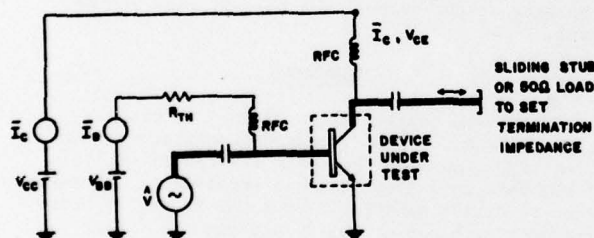


Figure 1A Microwave Rectification Response Test Set-Up for a Transistor

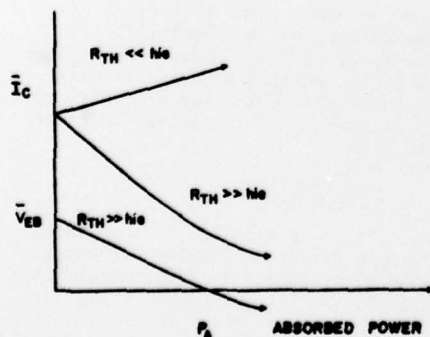


Figure 1B Rectification Response Showing Change in Average Collector Current and Emitter Base Voltage Due to Absorbed Microwave Power.

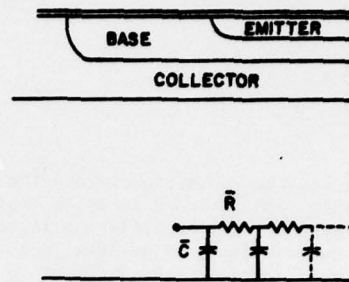
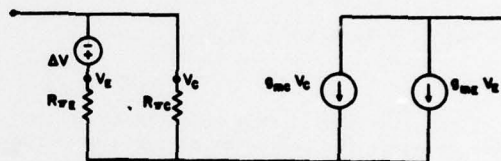


Figure 2 Profile of Bipolar Transistor and RC Transmission Line Equivalent Circuit for Calculation of Microwave Voltage Distribution



$$R_{VE} = \frac{V_T}{I_0} \frac{\beta_E + 1}{(X)}$$

$$g_{mc} = a_c \frac{I_0}{V_T} X$$

$$R_{VC} = \frac{V_T}{I_0} \frac{\beta_C + 1}{(1-X)}$$

$$g_{mc} = a_c \frac{I_0}{V_T} (1-X)$$

$$I_C = g_{mc} V_C + g_{mc} V_E$$

$$\Delta V = \frac{q}{\sqrt{2}kT} \sqrt{\frac{A}{W_0} \cdot \frac{A}{\omega C_T} \cdot \frac{1}{P_E} \cdot P_A^2}$$

Figure 3 Rectification Response Equivalent Circuit for Bipolar Transistor Circuit Analysis

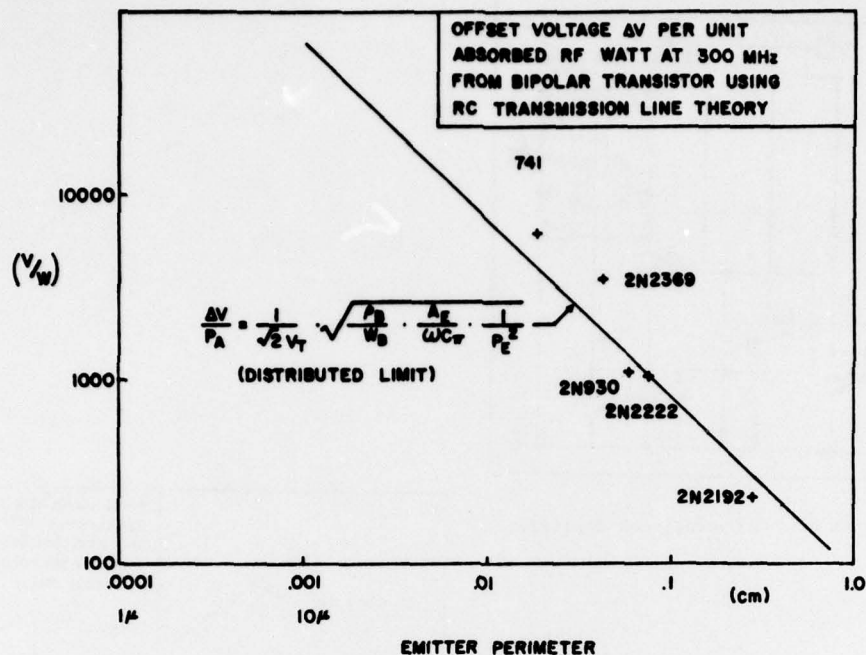


Figure 4 Rectified Offset Voltage Sensitivity Factor vs Emitter Perimeter for Bipolar Transistors using Typical Doping Parameters

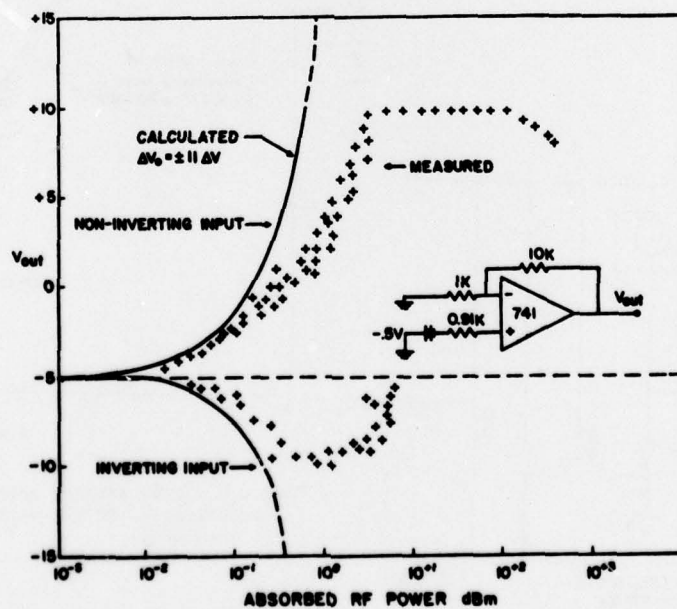


Figure 5 Behavior of 741 Op-Amp Output Voltage When Microwave Power is Injected onto the Inverting or Non-Inverting Input Ports

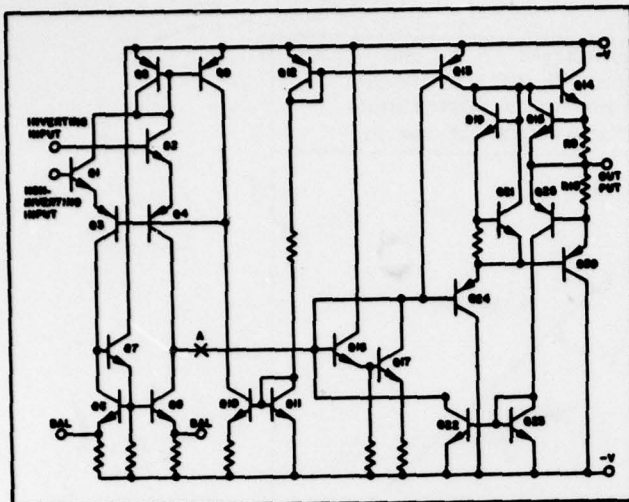


Figure 6 Schematic Diagram of 741 Operational Amplifier

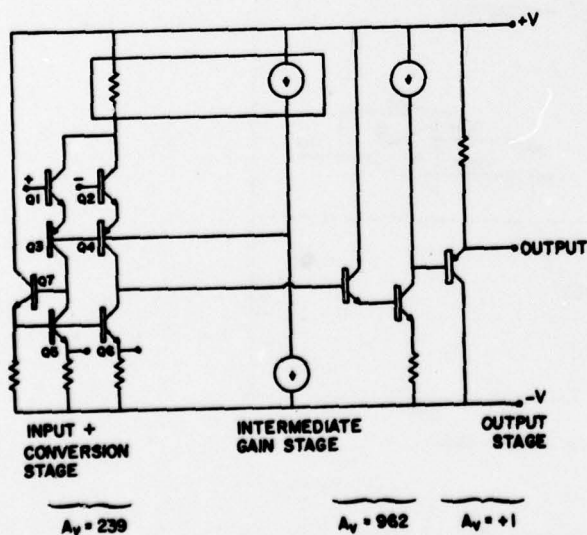


Figure 7 Simplified Schematic of 741 Operational Amplifier for RFI Analysis Purposes

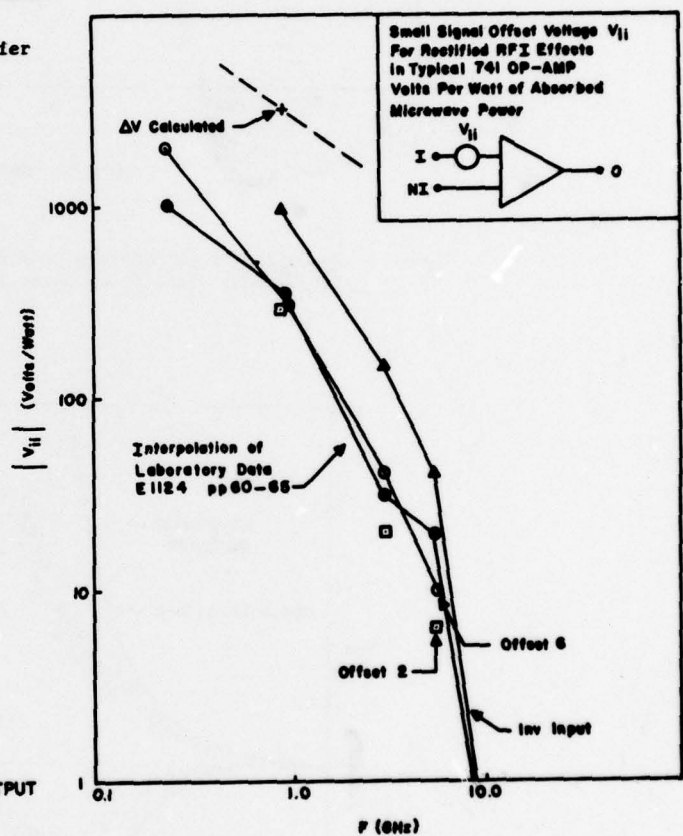


Figure 8 Comparison of Measured and Calculated Rectification Offset Voltage per unit Absorbed Power vs Frequency